

IMPROVEMENT OF THE TAROT SYSTEM USED FOR SPACE DEBRIS OPTICAL OBSERVATIONS AND OBSERVATION CAMPAIGN RESULTS

S. Ríos Bergantiños⁽¹⁾, B. Deguine⁽²⁾, A. Klotz⁽³⁾, C. Thiebaut⁽²⁾, J. Foliard⁽²⁾, M. Boër⁽⁴⁾

⁽¹⁾Expectra, Toulouse (France), ⁽²⁾CNES, Toulouse (France), *beatrice.deguine@cnes.fr*, ⁽³⁾CESR, Toulouse (France), ⁽⁴⁾Observatoire Haute Provence, Saint Michel (France)

ABSTRACT

Precise knowledge of the satellites and debris in the vicinity of the Geostationary Earth Orbit (GEO) arc and high-altitude regions is necessary to improve our knowledge of this population in order to preserve these regions for the future. The Rapid Action Telescope for Transient Objects (TAROT) is used to detect and track objects of a given minimum size orbiting in high-altitude and GEO regions. This telescope has two major advantages: an autonomous capability and a remote control with a real time processing capability and a large field of view that enables a systematic survey of the high-altitude and GEO regions to detect and track both catalogued and uncatalogued objects. Since January 2004, French National Space Agency (CNES) participates in the Inter-Agency Space Debris Coordination Committee (IADC) observation campaigns with this instrument. Since then, several major improvements have been brought at different system levels as for instance the modification of the telescope scheduler in order to quickly re-observe a new detected object or the image processing software improvement in order to detect and track smaller objects. This paper presents briefly the observation system, then all the major modifications brought in the system, the debris observation mode and associated data processing, and the observation campaign results obtained to test these modifications. The on-going work with the described system is also discussed.

1. INTRODUCTION

The geostationary orbit is becoming more and more cluttered as it offers numerous advantages for many applications. Precise knowledge of the satellites and debris in or near the geostationary arc and high altitude regions as the Medium Earth Orbit (MEO) one is necessary to define guidelines to protect those regions, and to verify their application. Ground based telescopes offer a satisfactory solution to the geostationary and high altitude population knowledge acquisition problem.

The CNES uses the TAROT telescope to observe the GEO and high altitude regions and to participate in the IADC GEO campaigns. This instrument is well-suited to the debris observation firstly because of its wide field of view which makes the detection and tracking easier; secondly because of its automatic scheduler which allows remote control and preparation of work plans to be run later; thirdly because of its agility which allows observations of lower orbit objects. The use of a star catalogue makes it possible to determine the telescope pointing to a high level of precision, and thus to obtain position data for the observed object. Detection of small

size objects is possible as photons from the observed object are cumulated on the same pixel of the CCD array during the exposure time.

This paper firstly presents briefly the TAROT telescope and its main characteristics, secondly the major improvements brought to the telescope scheduler. Thirdly, it describes the image processing software modifications. Finally, some results of these 2004 IADC campaigns are presented.

2. THE TAROT OBSERVATORY

TAROT is installed on the Calern plateau above Grasse in the South of France and belongs to the National Scientific Research Centre (CNRS). Its primary goal is the observation of optical counterparts of Gamma Ray Burst.

It is equipped with an equatorial mount and a primary mirror of 25cm diameter. TAROT is fitted with a Marconi 42-40 thin CCD camera with a size of 2048×2048 pixels whose size is 13.5 μm – 3.2 arcseconds. The readout time is 5s and the readout noise is 8.5e-. The resulting field of view is 1.86deg × 1.86deg. The system can detect 17th magnitude stars in a 10 seconds integration time. Due to its primary mission, this telescope has to be agile: the slew-speed is of 80deg/sec in both directions.

The robot system software is constituted of four parts:

- The multi-users web interface which manages the observation requests.
- The request scheduler which computes the telescope scheduling according to priorities and quota associated to each user.
- The hardware action scheduler which manages the telescope pointing, the camera, the weather forecast and the alarms.
- The image processing which carries out the suitable treatment (dark corrections, flat, sources extraction, specific treatments for each user, files stocker).

3. TELESCOPE SCHEDULER

The telescope scheduler has been improved for many reasons which are briefly given hereafter:

- The scheduling was computed at a fixed hour everyday. This implies that, during the night, it wasn't possible to add new observation request to track a newly detected object which hasn't been identified with the United States Strategic Command (USSTRATCOM) debris catalogue.
- The scheduler wasn't able to correctly deal with the user priority and the user observation quota which

represents a percentage of the night time allowed to take images for each user.

- The scheduler algorithm wasn't optimal in the sense that there were a lot of remaining telescope inactivity time periods during the night and several observation requests for the current night weren't planned.
- Some geometrical constraints such as the minimum height above the horizon, the minimum distance from the Moon and so on, couldn't be taken into account until now.

Let's first define the term request. One request is constituted by one or several observation sets. Each set consists of one position expressed in Right Ascension (RA) and Declination (Dec) coordinates, a telescope drive speed expressed in (X,Y) axis and a serie of six exposures maximum. Moreover, additional constraints such as the first exposure time can be defined.

The scheduling consists in building the list of observation sets of the current or future night. The major steps of this new algorithm are briefly summarised:

- Firstly, the observation sets which can't be observed during the night are eliminated.
- Secondly, the observation sets are sorted according to their priority. In case of a same level of priority, the priority is given to the observation set that must be observed the first due to geometrical sky conditions.
- Thirdly, the sorted observation sets list is scanned several times in order to get an optimised list with respect to priority, time conflicts and quota.
- Finally, if there are still telescope inactivity time periods, some observation sets that have been previously eliminated due to quota reasons for instance can be taken into account by allowing a quota overflow. Then, if all observation sets have been scheduled and there is still time free, some sets are duplicated and scheduled. This last step is only interesting for scientific applications not for the space debris one.

The scheduling is calculated every time a new observation request is sent. It lasts from 40 to 200 seconds on a 3 GHz / 512 Mo computer depending on the CPU load due to the fact that the computer deals with other activities. The telescope inactivity time periods usually represent less than 5% of all the night.

The advantages of this new scheduler are given below.

- The scheduling is computed each time a new observation request is sent.
- The user name is now written in the requests which allows a easier management of the archive.
- More observation constraints, as the minimum height above the horizon for instance, can be used.

But, there are still some improvements to implement.

- The scheduler doesn't take into account the status of the images. It means that if the images scheduled at the beginning of the night for instance weren't taken due to weather conditions, the scheduler doesn't plan them again later in the same night.
- It is necessary to link the couple (request, scheduling) with a database that contains all the observation requests and the images status in order to optimise the scheduling.
- The scheduling computation takes too much time to be used in a real time context. A real time work requires two scheduling steps: a mean term one at a scale of a few hours and a long term one.

The new scheduler has already been implemented in the TAROT system and is under final validation.

4. IMAGE PROCESSING SOFTWARE IMPROVEMENT

This section presents the detection and tracking algorithms for space debris observation. The "prototype" algorithms, which have been used during the 2004 GEO IADC campaigns weeks, were implemented in October 2003. The prototype algorithm performances are weaker than the expected ones in terms of reached limit magnitude for example. It only allows to detect automatically GEO objects. This is why a new detection algorithm has been developed. In addition, a new tracking algorithm has been defined and implemented to bound the false detections generated during the detection phase. These new algorithms will allow to detect automatically GEO objects and GEO transfer Orbit (GTO)/Highly Elliptical Orbit (HEO) objects near their apogee. The detection of LEO, MEO objects or GTO/HEO objects far from their apogee can be solved by using the Hough transform method.

4.1. Detection Algorithm

Until now, the detection threshold was a fixed value around 200 ADUs (Analogue Digital Unit) to avoid generating too many false detections. By using such a value, two major drawbacks can be mentioned:

- The algorithm is limited in terms of magnitude and so it prevents from detecting small size objects.
- This threshold is unsuitable because the image background noise depends on the observation conditions (full Moon...)

The updated method is still based on the last detection algorithm described in the following article (Boër, 2004) but the detection threshold is now varying as a function of the image background noise level. The image background noise is the standard deviation of the image histogram after applying iterative cuts on it around its mean value. Thus, the detection threshold is equal to k times this standard deviation.

To determine the optimal k value which represents a compromise between the algorithm sensitivity and the number of generated false alarms, different images, taken over one-month period with different Moon

phases and with satellite whose magnitude decreases along the night until it becomes invisible, were processed. Thanks to this study, the constant k has been set to 8.

This new detection threshold is then used to process again the data of the 2004 January campaign. New objects have been detected, but more false detections have been generated by the existing tracking algorithm as it isn't enough robust. Due to this last statement, a new tracking algorithm has to be developed in order to decrease the number of false alarms at the end of the process. This is the goal of the next section.

4.2. Tracking algorithm

The tracking algorithm is used after the detection algorithm to minimise simultaneously the number of false detections generated at the previous step and only keep the objects whose evolution corresponds to a GEO, GTO/HEO objects.

Several algorithms have been studied and the selected one is based on the B. Vandame's algorithm, which is an adaptation of H. Scholl's algorithm for the identification of quick asteroids (Bijaoui, 1999).

4.2.1 Algorithm principle

Its main idea consists in correlating different measurements in order to keep only at the end the objects seen over 3 images at least (against 2 for the existing algorithms). The images are pre-processed and calibrated with a star catalogue during the automatic process and therefore the relative positions (RA,Dec) from one image to the next are correct. The algorithm is described hereafter.

1. Object selection in the debris candidate file coming from the detection algorithm by processing the image taken at t_n .
2. Search of the k objects contained in the search window $n^{\circ}1$ of the debris candidate file obtained at t_{n+1} . We get a set of lists L_k composed of doublets (two positions (RA₁, Dec₁) and (RA₂, Dec₂)).
3. For each list L_k :
 - a- Initialisation of the variable $index=2$
 - b- Calculation of the velocity vector between the two last points of each list.
 - c- Estimation of the object position in the debris candidate file obtained at $t_{n+index}$
 - d- Search of the objects in the search window $n^{\circ}2$ in the debris candidate file at $t_{n+index}$ around the predicted point.
 - e- If an object is found, it is added to the list L_k that contains an additional position (doublet, triplet and so on)
 - f- Add 1 to the variable $index$
 - g- Go back to 3b whenever a debris candidate file exists
4. Each list L_k is a trajectory of at least 2 points.
5. The objects belonging to a given trajectory can't be candidates for another.
6. Loop on all the objects of all debris candidate file.

Note:

- If any object isn't found in the search window $n^{\circ}2$ around the extrapolated position at t_2 , we go to the next image.
- The time window over which the correlation process is run is short in order to be able to assume a linear trajectory of the object in the (X,Y) or (RA,Dec) plane. It will be useful for position prediction method (see later in the article).

Fig. 1 illustrates the algorithm: an object is found in the search window n° at t_1 , so the positions can be predicted in the future. No object is found in the search window $n^{\circ}2$ around the predicted position at t_2 : the next image is selected. On the image taken at t_3 , an object is found in the search window $n^{\circ}2$.

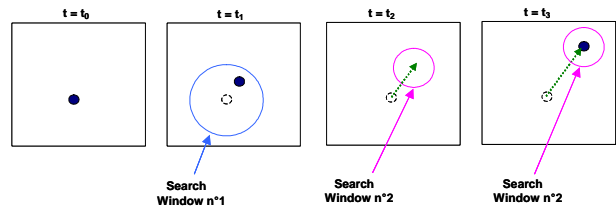


Figure 1: Implementation of the algorithm.

The drawback of this algorithm is that the debris candidate should be detected on 3 images in order to keep it.

4.2.2 Algorithm Parameters

The use of this algorithm under a linear evolution hypothesis needs the adjustment of three parameters described below.

• The maximum time window over which measurements correlation is done

In 10 minutes, the object trajectory can be assumed as linear in the (RA,Dec) plane whatever orbit is. Moreover, this time is slightly greater than the time needed by a GEO object to cross the field of view of TAROT. So, the time window over which the measurements correlation is run, is set to 10 min.

• Size of the search window $n^{\circ}1$

This algorithm is able to deal with different kinds of orbits:

- Geosynchronous orbit whatever inclination is
- Transfer GTO orbit or very elliptic (HEO)

After considering different orbits and analysing for each of them the separation angle between two consecutive positions obtained at around 30-40 seconds time interval with TAROT, the search window $n^{\circ}1$ size is chosen equal to 300 arcsec or 0.08 degree.

• Size of the search window $n^{\circ}2$

The tests done on the TAROT measurements of GEO and GTO objects have shown that the maximal error between predicted and observed positions is of the order of several 10^{-3} deg. So, the search window $n^{\circ}2$ size is chosen equal to 36 arcsec or 10^{-2} deg.

4.2.2 Algorithm implementation

Fig. 2 presents the general algorithm that has been implemented.

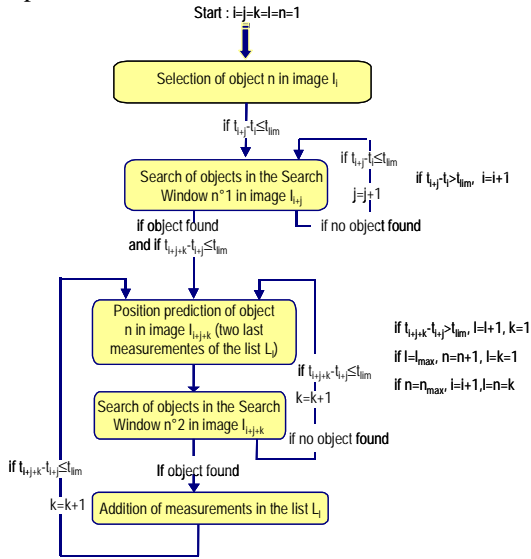


Figure 2: General Algorithm

At that time, this algorithm is under validation and will be used to process again the 2004 IADC campaign data.

4.2.3 Position prediction

Let's consider the geocentric coordinates (RA,Dec). The position of the third measurement must be extrapolated from two initial measurements.

Let t_1 , t_2 and t_3 be the three successive times of the measurements. At time t_i , the position of the object is (RA_i, Dec_i) . Let d_{ij} be the distance between the measurements at t_i and t_j . By assuming a linear trajectory and a constant velocity, one get Eq. 1 and Eq. 2.

$$RA_3 = RA_2 + \frac{t_3 - t_2}{t_2 - t_1} \times (RA_2 - RA_1) \quad (1)$$

$$Dec_3 = Dec_2 + \frac{t_3 - t_2}{t_2 - t_1} \times (Dec_2 - Dec_1) \quad (2)$$

Table 1: CNES 2004 IADC campaigns results

	18-24 Jan 2004	17-23 March 2004	16-22 April 2004	11-17 September 2004
Obs. Time	3 nights / 16h50 (7 nights / 42h) (+2h15: LST+1h)	5 nights / 26h34min (7 nights / 54h)	4 nights / 17h (7 nights / 42h) (+4h: LST+1h)	6 nights / 32h30min (7 nights / 37h)
Scanned area	505 deg² (+67.5deg ² : LST+1h)	797.10 deg²	510 deg² (+120deg ² : LST+1h)	978 deg²
Frames	2045 (+270: LST+1h)	3191	1810 (+480: LST+1h)	2838
Cor. Detect.	41 (of which 5 GTOs)	131 (of wich 19 GTOs)	74 (of wich 11 GTOs)	105 (of wich 15 GTOs)
Uncor. Detect	16 (of which 4 GTOs)	39 (of which 10 GTOs)	19 (of which 2 GTOs)	93 (of which 17 GTOs)

5.2. Identification with the debris catalogue

The identification with the USSTRATCOM catalogue provides error position between equatorial topocentric coordinates smaller than or equal to 50 arcseconds for 42% of the correlated objects. In fact, the reference

Remark:

- This relation should be the same in (X,Y) planes or (HA,Dec) plane. HA refers to Hour Angle.
- If a new measurement is found close to the predicted position, it is added to the list of measurements of the debris candidate. To have a better accuracy, the two last measurements of the list must be used to predict the next position.

5. 2004 GEO IADC CAMPAIGNS RESULTS

During 2004, CNES participates in the four weeks of IADC observation campaigns with TAROT. The results given here have been obtained with the old algorithms.

5.1. Observations

Fig. 3 presents the observed fields during the four weeks of campaign.

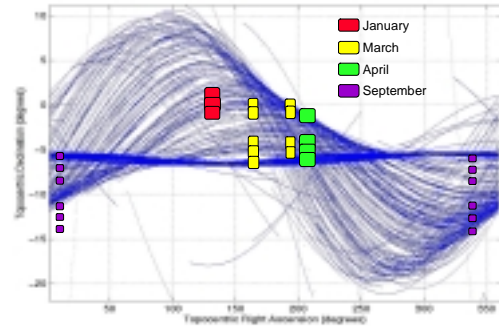


Figure 3: Survey fields of the IADC 2004 GEO campaigns observed by the CNES in the topocentric (RA,Dec) plane

Tab. 1 summarizes the observation times, scanned area, number of frames, number of correlated and uncorrelated detections (Correlated Target - CT or Uncorrelated Target- UCT) for each week. The number of uncorrelated detections is high; this is due to the USSTRATCOM catalogue which is incomplete and not often updated for GEO objects.

LST = Local Sidereal Time

catalogue is not enough frequently updated to provide precise Two Line Elements.

The comparison between observed and extrapolated (by using USSTRATCOM catalogue) positions for correlated objects leads to good results. The comparison of inclination values leads to a mean error equal to

0.037 deg for GEOs and 0.168 deg for GTOs. The instantaneous longitude and the semimajor axis for GEO objects are also well estimated: the mean error for the instantaneous longitude is around 0.068 deg for GEOs and 0.024 deg for GTOs. The mean error for the semimajor axis depends on the pointed geocentric declination: for instance, it is equal to 90km for the 3 nights of January ($Dec_{GEO} = 7.8, 6$ and 4.2 deg) and to 10km for the 21th April ($Dec_{GEO} = -1.2$ deg).

Note:

The instantaneous longitude is defined by Eq. 3.

$$long_{inst} = \arctan\left(\frac{y}{x}\right) - \theta \quad (3)$$

where θ is the sidereal time and (x,y,z) are the coordinates of the Earth centre/satellite vector and are associated to one given measurement.

5.3. Orbital parameters and magnitude distribution

The distribution of orbital parameters is a simple way to show the observed population characteristics. Fig. 4 presents the inclination distribution: the 0 deg-inclined orbits were well observed, as well as the ones centred at

6 and 8 deg of inclination. Objects orbiting on a high inclination trajectory (more than 15 deg) were also well detected: these objects designated as GTO objects are actually geosynchronous ones. The 4 objects after 20 deg are GTO-CTs.

The orbital plane (i,Ω) is used to discriminate GEOs from GTOs (see Fig. 5): indeed, the orbital planes of uncontrolled GEO objects exhibit precessional motion so that their plane inclinations vary periodically (with a period of 53 years) from 0 to 15 degrees (Schildknecht, 2002). The precessional motion is responsible of the correlation between the inclination and the Right Ascension of Ascending Node parameters (RAAN). One can see this orbital plane behaviour on Fig. 5 by having a look at the distribution from 0 to 15 degrees for inclination and 0 to 100 degrees for RAAN. As we said in section 5.1, some of the wrongly noted GTOs complete this distribution from 10 to 15 deg: they are geosynchronous inclined objects. Some GTO objects as well as uncorrelated GEO objects whose inclination is between 0° and 15° don't seem to follow this behaviour. So, one can't conclude about the GEO/GTO discrimination by using this distribution.

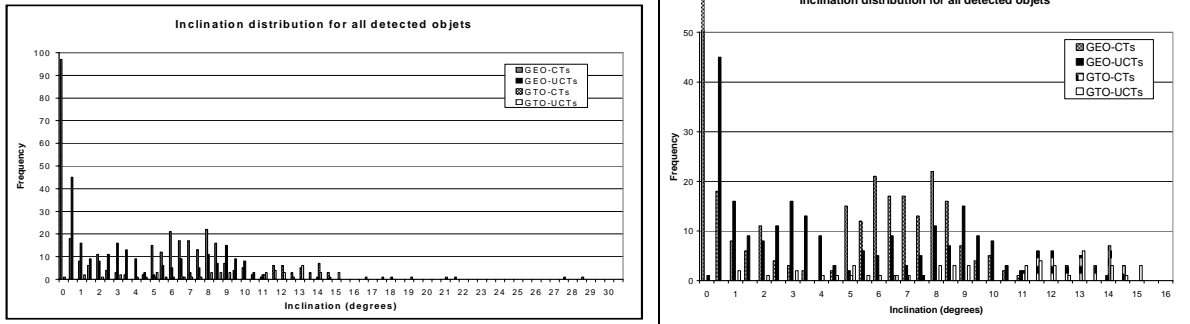


Figure 4: Inclination distribution for all the detected objects during the four weeks of campaign.

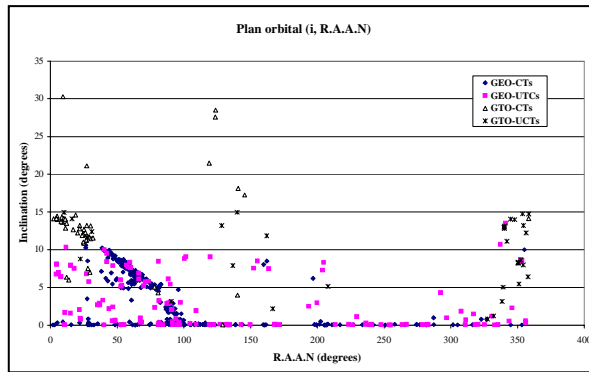


Figure 5: Orbital plane (i,Ω) obtained after the four weeks of campaign.

The corrected magnitude distribution is presented on Fig. 6. The instrumental magnitude is corrected thanks to calibration stars (Landolt stars) observed all through the night. The median value of the differences between instrumental and catalogue magnitude provides the correction. No phase angle correction is applied. The detection prototype algorithm provides a magnitude distribution centred on the 11th magnitude, which is equivalent to a size of 7m on the GEO arc, assuming a 0.2 albedo. The maximum detected magnitude is 15

which represents an object size of 1m in the GEO arc (with a 0.2 albedo). The correlated and uncorrelated GEO and GTO objects are distributed in a similar manner except that the biggest detected objects are uncorrelated ones. The detection prototype algorithm implies a limited detectable size associated to satellites or large debris such as rocket bodies. The observed peak corresponds to the first peak of the bimodal distribution observed by ESA (Schildknecht, 2002).

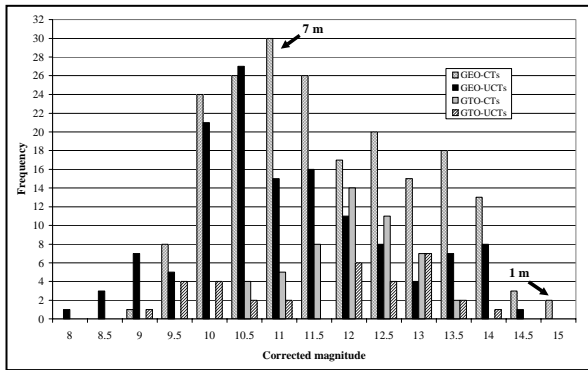


Figure 6: Corrected magnitude distribution for the detected objects.

5.4. Other observations

During the March and April campaigns, we have also detected MEO objects. Actually, the geometrical configuration station/satellite/Sun was more favourable to these detections in March and April than in January and September. If these objects were observed on at least two frames, their direction was known and a preliminary orbit determination was made; 19 MEO objects were detected and 14 were identified with the USSTRATCOM catalogue during March and April campaigns. They were all GLONASS satellites or GLONASS upper stages. During the April campaign, GTO objects were also observed far from their apogee and so with a higher speed motion: 4 objects of this nature have been detected and 2 have been identified with the USSTRATCOM catalogue. They don't appear as point source on the frames but as streaks that could be as long as the MEO ones.

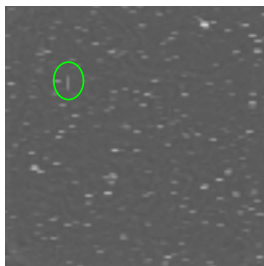


Figure 7: TAROT image of a MEO in 2004 March campaign.

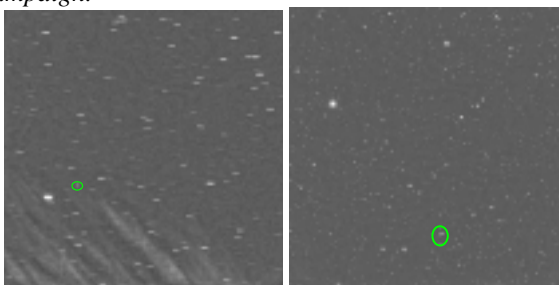


Figure 8: TAROT image of Rosetta (4/3/2005) in GEO mode (left) at an altitude of 61665 km and tracking mode (right) at an altitude of 24657 km. Magnitude 9.7.

During the 4th March 2005 night, Rosetta probe came close to the Earth and thanks to TAROT, several images were taken in two different modes as shown in Fig. 8:

- a GEO mode used when the object is at an altitude higher or equal to the geostationary one: the object is fixed and the stars are represented by streaks,
- a tracking mode used when the object altitude is smaller than the geostationary one : the stars are represented as points and the object is described by a streak.

CONCLUSION

New detection and tracking algorithms have been defined and developed in order to be able to detect faint objects whose magnitude can reach the instrument limit one, to detect automatically geosynchronous and GTO/HEO objects near their apogee, to allow to quickly re-observe newly detected objects several minutes later and to correctly deal with user priority and observation quota and constraints thanks to the new scheduler.

The results presented in this paper show that TAROT is well suited for space debris survey as well as for target tracking due to its characteristics. Moreover, TAROT is able to track LEO objects due to its slew-speed. For instance, SPOT5 was tracked by TAROT during April 2004.

ON-GOING WORK

The validation of the scheduler and the image processing are under work and should be finished by the end of summer 2005.

In order to work in real time, the TAROT scheduler will have to be re-designed by probably using two scheduling steps : a mean-term and a long-term ones. This work should start around September 2005.

Moreover, these algorithms will have to be extended in order to process automatically LEO and MEO objects.

In addition, an user interface named MADEOS is under development so that the whole process of observation request generation, request transmission to TAROT, object identification, position computation and object database management will be automatic. This work is under progress.

REFERENCES

Bijaoui A., Cokelaer T., Maury A., Vandame B. *Détection des débris spatiaux – Rapport final* – 8 Septembre 1999.

Schildknecht T., Musci R., Ploner M. and al., *Optical Observations of space debris in GEO and in Highly-eccentric orbits*, PEDAS-B1.4-0007-02, 34th COSPAR Scientific Assembly, Houston, Texas, USA, Oct 10-19, 2002.

Thiébaud C., Klotz A., Foliard J., Deguine B., Boër M., *CNES optical observations of space debris in geostationary orbit with the TAROT telescope: IADC campaign results*, COSPAR 04-A-00984, Paris, 18-25 July 2004.

Boër M., Klotz A., Thiébaud C., Foliard J., Deguine B., Alby F., *Monitoring the geostationary orbit with TAROT*, COSPAR 04-A-01205, Paris, 18-25 July 2004.